

Post-print version of the article published in:

Journal of the Optical Society of America A, 31, A375-A384

© 2014 Optical Society of America. One print or electronic copy may be made for personal use only. Systematic reproduction and distribution, duplication of any material in this paper for a fee or for commercial purposes, or modifications of the content of this paper are prohibited. URL: <http://dx.doi.org/10.1364/JOSAA.31.00A375>

Variation of color discrimination across the lifespan

Galina V. Paramei* and Beata Oakley

*Department of Psychology, Liverpool Hope University, Hope Park, L16 9JD Liverpool,
United Kingdom*

** Corresponding author: parameg@hope.ac.uk*

RUNNING HEAD: Cambridge Colour Test measures across the lifespan

Abstract

The present study, an extension of Paramei (J. Opt. Soc. Am. A, 29, A290, 2012), provides normative data on chromatic discrimination, using the Cambridge Colour Test, for normal trichromats aged 10–88 years. Findings are in accord with a two-phase variation across the lifespan: chromatic sensitivity improves in adolescence, reaches a maximum around 30 years, and then undergoes a gradual decrease. Indicative parameters are Protan (P), Deutan (D) and Tritan (T) vector lengths; and major axes and axis ratios of Ellipses. Trivector data are modeled as non-monotonic combinations of power functions, with goodness-of-fits $R^2_P=0.23$, $R^2_D=0.23$, $R^2_T=0.45$. For advancing age, sensitivity decline in all chromatic systems was confirmed, though with a marked acceleration after 60 years (reflected by the power function exponent > 1) and more pronounced for the Tritan system.

OCIS codes: 330.1690 Color; 330.1720 Color vision; 330.4300 Vision system - noninvasive assessment; 330.5020 Perception psychology; 330.7323 Visual optics, Aging changes; 330.5510 Psychophysics

1. INTRODUCTION

Color vision varies across the lifespan. There is a consensus that in color discrimination tasks, performance reveals a two-phase variation [1-3], with thresholds following a U-shape function with age [4,5]. In particular, from early childhood through adolescence, chromatic sensitivity becomes progressively better, reflecting maturation of the visual system [2,4-7].

In late adolescence–young adulthood, chromatic discrimination thresholds reach their minimum, with troughs reported to fall around 20-24 years [1] or 19 years [5] (Farnsworth Munsell 100-Hue test); 20-29 years [3] (Lanthony Desaturated Panel); 18-21 years [4] (Colour Assessment and Diagnosis test); or in the (less specified) range of 18-30 years [7] (Cambridge Colour Test).

Beyond the U-trough, a more gradual aging trend begins, manifesting as a generalized increase in chromatic thresholds. After 40 years, the aging effect was reported to increase with each life decade and accelerate beyond 60 years, as well as become increasingly variable among healthy normal trichromats, in particular beyond 60 years [8,9].

The causes and loci of the chromatic sensitivity decline are multiple: senescent changes occur in the ocular media, at the photoreceptor level and higher in the visual system [10]. In the periphery of the visual system, age-related losses are predominantly caused by increasing density and yellowing of the crystalline lens, which progressively filters light transmission, especially at shorter wavelengths [11-15]. Further, there is evidence of continuous and parallel decline in sensitivity in all chromatic systems, as measured by performance on color vision tests, with especially pronounced decline along tritan axes [4,8,15-18]. Along with the negative impact of the lens brunescence, the deterioration of chromatic sensitivity is attributed to losses in spectral efficiency of short (S-), middle (M-), and long (L-) wavelength cones [16,19-24]. There is less agreement though whether losses in sensitivity of M- and L-cones occur at the same rate as in more vulnerable S-cones.

In focus here are changes of discriminative capacity in normal trichromats (NTs) across the lifespan, as measured by the Cambridge Colour Test (CCT) [25]. As a computer-controlled test, the CCT allows precise control of chromaticity parameters of the figure and the background (defined in the CIE 1976 $u'v'$ chromaticity diagram), and multiple randomised presentations of the figure–background chromaticity differences. A psychophysical method for estimating discrimination thresholds allows a rapid testing procedure and provides a quantitative outcome that is sensitive to individual differences among NTs, distinguishes the latter from color abnormal observers, separates protans and deuterans well and reveals the large range of chromatic sensitivities among anomalous trichromats [25,26].

The CCT includes two tests: a Trivector test enables the estimation of discrimination thresholds along the Protan, Deutan and Tritan confusion lines, to emphasize the contributions to sensitivity of the L-, M-, and S-cones, respectively. An Ellipses test determines three MacAdam ellipses [cf. 27] with their centers located at intervals along the same tritan confusion line.

In the present study we measured color discrimination thresholds in a representative sample of healthy normal trichromats of the age range spanning eight life decades, 10–88 years. It is an extension of work by researchers from Brazil, for a population aged 18–30 years old [28], and of our own work for four life decades (20–59 years) [29].

The aim of this study is to provide normative data for the CCT for each of the eight life decades [cf. 5]. Note that in clinical studies of mature patients, the CCT is used for assessing chromatic discrimination loss, an early manifestation of a developing ocular or systemic disease, and thus for diagnostic and monitoring purposes [cf. 30-38]. Keeping in mind that in some of these studies the age range of patients and matched controls spanned from two to four life decades, it is highly probable that the mean values for the compared

groups include a contribution from the aging effect in individual observers. The reference estimates provided here will enable direct comparison of the patient's outcome with that of healthy normal trichromats of the corresponding life decade.

In addition to this applied research objective, we questioned which life decade would reveal initial sensitivity decline along each of the Protan, Deutan and Tritan confusion lines linked to the L-, M-, and S-cone systems, respectively. We also addressed two propositions ensuing from the previous studies of variation of chromatic sensitivity, specifically, (i) U-shape function of discrimination thresholds across the lifespan [4,5] and (ii) the putative parallel and comparable decline in sensitivity of all chromatic systems with advancing age [4,8,15-18].

2. METHODS

A. Subjects

The observers were aged 10–88 years old and had normal or corrected-to-normal vision. To ensure normal trichromatic vision, prior to the experiment all subjects underwent color vision diagnostics using the Ishihara Pseudoisochromatic Plates [39], to screen for congenital red-green deficiency, and the Farnsworth Dichotomous Test (D-15) [40] and the Lanthony Desaturated Panel (D-15d) [41], for assessing color discrimination ability.

From a total of 423 participants tested, data of 291 healthy color normal trichromats were included in subsequent analysis. The dataset for participants aged 20–59 years (N=160) is identical to that in [29]. The number of participants, gender split and age details for each life decade are given in Table 1.

Data were excluded from those participants who self-reported congenital color abnormality, history of ophthalmological pathology (ocular/retinal disease), cataract (pre- or post-surgery treatment), diabetes, or neurological diseases. In addition, data were excluded

from observers with monocular vision, since binocular color discrimination has been reported to exceed monocular performance [2], and from those who wore tinted glasses/lenses known to affect chromatic discrimination [42]. Further, from non-daltonic subjects, data were excluded from those participants (N=18) who underperformed on the D-15 and/or D-15d tests (as a rule, multiple transpositions, with transposition values 3 or greater). Among the excluded non-daltonic cases more than half (N=85) fell into the four later age decades, 50-88 years, predominantly due to diabetes, glaucoma and cataract (surgery).

Participants were Psychology students of Liverpool Hope University, who participated against credit points; and staff members, acquaintances, or members of the local community, rewarded £10 for their participation. Ethical consent was obtained from the Ethics Committee of the Psychology Department, Liverpool Hope University, before conducting the study.

B. Apparatus

For chromatic discrimination testing, the Cambridge Colour Test, v1.5, was used [Cambridge Research Systems Ltd. (CRS), Rochester, UK; Ref. 43]. Implementation and calibration procedures were performed with software and hardware provided by the CRS (OptiCAL; VSG interface version 8.12; graphics card VSG 71.02.01E9). Stimuli were presented on a high-resolution gamma corrected 21 inch color monitor (Mitsubishi Diamond Pro 2070SB).

C. Stimuli

The CCT stimulus is a pattern of distributed small circles randomly varying in size and luminance (8, 10, 12, 14, 16, and 18 cd/m²). The target, a Landolt-like C-shaped ring, is defined by a superimposed chromatic contrast (Fig. 1). The ring chromaticity can be varied to differ from the background ($u' = 0.1977$, $v' = 0.4689$, CIE 1976 chromaticity diagram) by a

minimum excursion of 0.002 $u'v'$ units [25]. The gap in the 'C' opening subtends 1° of visual angle at the four-meter viewing distance. To identify the gap position, the subject is forced to use chromatic cues, since he/she cannot use spatial or luminance cues to infer the embedded shape.

Figure 1 about here

D. Procedure

Observers were dark adapted and tested binocularly; they were positioned at 4 m from the monitor. The target was presented with its gap randomized in one of four positions: up, bottom, right or left (4-Alternative Forced Choice). Participants were instructed to identify the gap position in the Landolt 'C' and press the corresponding button of the response box (CT6, CRS). Accuracy over speed was emphasized in the instruction. The response box was held by the subject with both hands, and the thumbs were used for button pressing. The time allowed for the subject to respond was 8 sec.

Chromatic contrast of the Landolt 'C' was varied relative to that of the background (in terms of the CIE 1976 $u'v'$ color space) [25]. The CCT uses a staircase psychophysical procedure to measure discrimination thresholds. Two interleaved staircases run in random order. Each staircase begins with a target of high saturation; the chromaticity of the target is then varied to reduce the contrast with the background. The step size and direction of the variation in chromatic contrast is contingent upon the subject's response, specifically: chromatic contrast is halved after a correct response and doubled following an incorrect response or no response (here: within the allocated 8 sec). Periodically, a control target at maximum saturation is presented. After six staircase reversals, chromatic discrimination

threshold (in $u'v'$ units) is computed as the average of the chromaticities corresponding to the reversals [25,26].

The CCT has two testing procedures, the Trivector test and the Ellipses test. The Trivector, a short (3-4 min) test, measures thresholds along the three confusion lines – Protan (P), Deutan (D), and Tritan (T) (Fig. 2a). The three corresponding pairs of staircases are run simultaneously, in an interleaved and random way. For young adult NTs, the P and D values do not exceed $100 \times 10^{-4} u'v'$ units, and the T values are no greater than $150 \times 10^{-4} u'v'$ units [25].

The Ellipses test maps three MacAdam ellipses in different sectors of the CIE $u'v'$ chromaticity diagram along a tritan line. Coordinates of their centers are as follows: Ellipse 1: $u' = 0.197, v' = 0.469$ (identical to that in the Trivector test); Ellipse 2: $u' = 0.193, v' = 0.509$; Ellipse 3: $u' = 0.204, v' = 0.416$ (Fig. 2b). The chromaticities are varied in relation to these references along either eight, 12, 16, or 20 vectors. The present study employed the eight-vector protocol (ca. 25 min), with vectors separated by 45° . After six incorrect responses or six reversals, thresholds along each vector are computed and used to construct an Ellipse using the method of minimum squares. Each Ellipse is defined by three parameters: Length of the major axis (in $u'v'$ units), Major-to-minor axis ratio, and Angle of the major axis (in degrees). For young adults, the axis ratio is typically less than 2 [25].

Figure 2 about here

After the instruction, the present study began an experiment with a practice session, for which a mock Trivector test was used to familiarize participants with the procedure and avoid misunderstanding. This practice session was followed by the Trivector test proper and the Ellipses test. In total, a session (including pre-experimental diagnostics) took 45-60 min for younger adults; it was longer, as a rule, for children and elderly observers, who required

more detailed explanations at the session outset and/or additional breaks in the Ellipses test.

3. RESULTS

A. Trivector test: Comparison of outcomes across the lifespan

Visual inspection of data and its descriptive analysis revealed that for all age bands the distributions were skewed. Therefore the following exploration of variation of chromatic discrimination uses nonparametric analyses, i.e., medians, with half-interquartile ranges (IQR/2) as the measure of dispersal.

Table 2 presents medians (\pm IQR/2) for P, D, and T vectors for the eight life decades. In addition, for each vector and age band we calculated upper and lower tolerance limits. The tolerance limits indicate a range of values for a measure, such that one may be 100(1- α)% confident that a given percentage of the population, from which the data sample was drawn, falls within that range. Since the data were skewed, nonparametric limits were calculated, which do not assume normality [45].

The STATGRAPHICS package [46], under the ‘distribution-free assumption’ and a ‘liberal criterion’, calculates tolerance limits which contain a specified percentage of the population; the probability that they do contain the percentage is also estimated, and depends on the sample size.

Following the lead of [28,29], we calculated tolerance limits for 90% of the population. For each of the six life decades, 10+ through 60+ (each N=40), the estimated probability is 92%. For the 70+ band (N=35), the estimated probability is 88%. However, due to the smaller size of the 80+ band (N=16) we opted for 80% tolerance limits, which provided 86% probability of including that percentage (the 90%-of-population validity was an inferior trade-off, providing a lower probability). These two exceptions are indicated in Tables 2–5 by * and **, respectively.

Table 2 about here

Fig. 3 shows natural logarithm (ln) of the chromatic thresholds as functions of age, measured along the Protan, Deutan and Tritan vectors. Note that Protan and Deutan functions follow similar trajectories; the corresponding graphs display two trends: (i) thresholds decrease between adolescence (10+) and the 20+ decade; (ii) beyond the minima of the functions, thresholds first increase at a modest rate, only to accelerate starting from 60 years of age. In comparison, thresholds along the Tritan vector hardly change between 10–40 years; beyond that, however, threshold elevation develops more rapidly, at particularly faster pace from 60 years. Tritan thresholds are also uniformly higher than Protan and Deutan, as is typically found for this color space representation ([4,7,18,28,29]).

We found that the data were fitted well by a nonlinear function combining two power functions:

$$T = \ln(aA^\alpha + bA^\beta) \quad (1)$$

where T is the logarithm of chromatic threshold, A the age in years (rescaled for convenience by dividing by 40), and a , α , b , and β are parameters [4,44]. Each pair of parameters is associated with one limb of the data, giving the limbs' slopes in ln-coordinates (α , β), and their intercepts (a , b). Parameters were fitted to the data using the `nls()` function of R (nonlinear least squares), with the natural-log transformation on both sides of Eq. (1) weighting variance equally across age. In Fig. 3, the fits obtained from Eq. (1) are shown as the black curves. Table 3 shows the values of the parameters, with standard errors in parentheses by each value, and the ages of minimal P, D, and T thresholds; the values of R^2 indicate the proportion of variance in the data accounted for by the fitted curves.

As indicated by Fig. 3 and Table 3, for all three functions the minima of chromatic discrimination thresholds fall around 30 years of age: $P_{\min}=30$ years, $D_{\min}=29$, and $T_{\min}=27$.

The troughs of the fitted functions are shallow, implying wide confidence intervals around these minima. Notably, in [4] the age of minimum T, 18 years, was again reported to be lower than P and D, both 21 years.

Two other models were also tested, with fewer free parameters, one assuming that α and β , the slopes of the two limbs, are shared across the three functions, P, D, and T, and the other implying that slopes of both limbs are equal, $\alpha = \beta$. However, according to an ANOVA comparison these models fitted the data significantly worse than that defined by Eq. (1).

Figure 3 and Table 3 about here

To explore the difference in Trivector outcomes between the life decades, nonparametric analyses of ln-transformed data were carried out, specifically, Kruskal-Wallis H test to assess the age effect across all life decades; followed by Mann-Whitney U test for pairwise comparisons between age bands, separately for the P, D, and T vectors.

Figure 4(a-c) about here

The age effect across the life decades was significant for all three vectors ($p < .001$): Protan, $\chi^2(7) = 57.07$; Deutan, $\chi^2(7) = 62.05$; and Tritan, $\chi^2(7) = 104.32$.

For *Protan* and *Deutan* vectors (Fig. 4a,b), pairwise comparisons revealed a significant threshold decrease between 10+ and 20+ age bands, followed by a further, though less pronounced decrease within the 20–29 band. Beyond 40 years, however, the P and D thresholds revert to a ‘creeping’ elevation; the increase becomes significant for the 50+ band, followed by the next elevation surge from 60 years.

For *Tritan* vector (Fig. 4c), any threshold decrease in adolescence or young adulthood is not significant in pairwise comparisons. The age effect is pinned down to the progress of

gradual threshold increase between 30–49 years, followed by considerable cumulative threshold elevation in the three consecutive decades beyond 60 years.

B. Ellipses test: Comparison of outcomes across the lifespan

All data obtained in the Ellipses test were, too, non-normally distributed, which required nonparametric tests. For each age band, medians (\pm IQR/2) and nonparametric tolerance limits are provided for the three Ellipses parameters – Length of the major axis (Table 3), Major-to-minor axis ratio (Table 4), and Angle of the major axis (Table 5).

Tables 4-6 about here

For further analyses, beyond the normative data, Kruskal-Wallis and Mann-Whitney tests were applied to ln-transformed data. For illustrative purposes, only outcomes for Ellipse 1 are presented graphically (Fig. 5).

Length of the major axis, the parameter that reflects discrimination along a tritan confusion line, was expected to behave similarly to the Tritan vector. Indeed, for all three Ellipses, age-related differences of the major axes were significant ($p < .001$): Ellipse 1, $\chi^2(7) = 129.5$; Ellipse 2, $\chi^2(7) = 148.5$; Ellipse 3, $\chi^2(7) = 38.56$. Pairwise comparisons of this parameter between age bands went further than those of the Tritan vectors (Fig. 5a): specifically, a significant major axis decrease in the 20–29 decade compared to the 10–19 band; benign but gradual increase between 40–59 years; and significant accruing increase beyond 60 years. Statistics (U) and values of significance for this parameter between the life decades for all three Ellipses can be found in Appendix (Table A1).

Figure 5(a,b) about here

Major-to-minor axis ratio, too, revealed a significant age effect ($p < .001$): Ellipse 1, $\chi^2(7) = 82.9$; Ellipse 2, $\chi^2(7) = 102.6$; Ellipse 3, $\chi^2(7) = 38.6$. Pairwise comparisons indicated that all Ellipses become larger after 50 years and, also more elongated with age, especially beyond 70 years (see Table A2). Noteworthy, under 70 years, median of the axis ratio varies between 1.29–1.46 for Ellipse 1 and 1.33–1.69 for Ellipse 2 (Table 4); the respective means of the medians, 1.38 and 1.44, are comparable to 1.56 reported in [26]. For Ellipse 3, median of the axis ratio varies between 1.86–2.27 across six life decades (from 10+ to 60+), with the mean 2.04 very similar to the ratio of 2 indicated in the CCT Handbook [25].

For the *Angle of the major axis*, a significant age-related effect was found only for Ellipse 1: $\chi^2(7) = 18.0$, $p = .012$. This outcome is apparently due to the Ellipse 1 being slightly rotated in two age groups, compared to the median 79° for all age groups: clockwise for the 20–29 band (67°) and counter-clockwise for the 70–79 band (86°) (Table 5). It is worth noting that the obtained range of Angle medians, 67° – 86° , is similar to the dominant range, 60° – 90° , reported for (the only measured) Ellipse 1 for a sample of control observers in earlier studies [32,47].

4. DISCUSSION

The indicative parameters for assessing variation of chromatic discrimination across the lifespan provided by the Cambridge Colour Test are lengths of all three vectors, Protan, Deutan, and Tritan (Trivector test); and Ellipse Major axes and Major-to-minor axis ratios (Ellipses test). Ellipses 1–3 were shown to vary in a similar manner with age; hence, in the future studies it is reasonable to constrain the testing procedure to one Ellipse (say, Ellipse 1), while increasing the number of the vectors from eight to 16 or 20 in the testing protocol, in order to achieve more precise fitting of an ellipse.

Over the lifespan, variation of the discrimination thresholds along the P, D, and T vectors is two-phase, following a U-shape function [cf. 1-5]. As in the study of Knoblauch et al. [4], our data for Protan, Deutan, and Tritan thresholds are best fitted by nonlinear, non-monotonic functions. Even so, the variances accounted for by these functions in our outcome, $R^2_P=0.23$, $R^2_D=0.23$, $R^2_T=0.45$, are much lower than the values reported in [4], 0.87, 0.84, and 0.87, respectively.

The discrepancy may be partly attributed to differences in the stimuli and protocol of the two tests employed, the Colour Assessment and Diagnosis (CAD) test in [4] and the CCT in the present study, specifically, a larger stimulus size (viewed from a distance of 57 cm) in [4]; higher background luminance, with mean luminance 34 cd/m^2 in [4], compared to $8\text{-}18 \text{ cd/m}^2$ in the CCT; as well as difference in the nature of luminance noise in the two tests, dynamic vs. static, respectively. Notably, Knoblauch et al. [4] remark that their pilot data indicated that a larger stimulus size and longer stimulus duration resulted in lower tritan thresholds. Recently a study was undertaken to assess a relationship between thresholds measured by the CAD test and the CCT, with preliminary results showing a high correlation between the two [48]. In the future it is worth exploring whether threshold measurements with dynamic stimuli (CAD test) are less susceptible to ‘noise’ in participants’ responses.

Also important for any least-squares function fitting are the differences in the age ranges. In the Knoblauch et al. study [4], observer sample ($N=172$) included a large proportion of very young infants (6–12 months old). In comparison, our sample, 10–88 years, included predominantly adult observers, with a relatively large proportion of those at the upper end of the age range. Since the latter manifest decline in chromatic sensitivity, this might have increased the variability in discrimination thresholds and, hence, reduced the R^2 values in the present study.

Another outcome in the data presented in our Fig. 3 is worth addressing: for all three functions, the minima are shallow and fall in the range of 20–40 years. The intermediate values, 27–30 years, are higher than the age minima found earlier: 20–24 years [1]; 18–21 years [4]; 19 years [5], or 18–30 years [7].

Note though that across these studies, the age range and observer proportion in each age cohort varied substantially. In particular, in Verriest [1], the age ranged between 10–64 years, with different observer numbers for (half-)life decades: {10-19 y.o.}: 105; {20-29 y.o.}: 145; {30-39 y.o.}: 70; {40-49 y.o.}: 62; {50-59 y.o.}: 69, and {60-64 y.o.}: 29 (see his Table II). In Knoblauch et al. [4], according to inspection of their Fig. 2, the observer sample (N=172) included 96 infants (under 1 year), a subsample (N=37) of children between 1-8 years, and an adult subsample (N=39) aged 16–64 years. Also Kinnear and Sahraie's [5] sample was dominated by younger observers, 5–22 years (N=328), compared to 50 adults, with 10 observers in each of the 30+ to 70+ decades (see their Table 1). Finally, Goulart et al. [7] related P, D, and T average thresholds for 2-7 year old children (N=25) to those of young adults (N=35), with mean age 21.8 years (range 18-30).

It is also noteworthy, that in their recent study Panorgias et al. [49] found that functions best fitting the CCT Trivector data variation with age (15–88 years) are linear for Protan and Deutan vectors and bi-linear for Tritan vectors, with the crossing point at 68 years for the latter. As in the discussion of the minima above, we venture to assume that their best-fitting function outcomes were affected by the lower extreme of the tested age range, 15 years, which lies near to the minima found in [4,5]. In addition, the “density” of observations between 15–20 years is low, compared to a very high “density” of observations between 20-30 years (see their Fig. 2).

The overview of the observer samples prompts a speculation that the shape of the fitting curve and the minimum in a U-shaped function are biased by the extremes of youth

and old age in a sample and, as well, by the evenness of the distribution of data on both sides of the minimum. It is conceivable that underrepresentation of the younger ages allows a linear function to fit the data, while a high proportion of data for very young, compared to that of data for adults, including elderly, biases the minimum to a younger age, as in [4,5]. To test this assumption, a simulation would be required, however.

Finally, we would like to comment on the differences in thresholds between individual life decades. The decrease of Protan and Deutan thresholds (Fig. 4a,b), pronounced between 10+ and 20+ and less apparent between 20 and 29 years (i.e., significant differences are revealed when comparing the 30–39 band's data to 10–19, but not to 20–29), is likely a manifestation of continuing maturation of the visual system into young adult age.

Contrary to our expectation, the performance of Tritan thresholds is different, hardly changing between 10 and 40 years (Fig. 4c). One may speculate that this is a manifestation of a counterbalancing of two processes with opposite dynamics, namely a non-optimal and slowly developing S-cone sensitivity is being outweighed by a very high lens transparency in younger ages. Some indirect evidence is provided in Wuerger [15] who calculated S-, M-, and L-cone absorptions throughout the lifespan from the lens model of Pokorny et al. [11]. Indeed, Fig. 2 in [15] indicates that in young ages (≤ 20 years), relative S-cone absorption exceeds that of M- and L-cones by about 20%, to then decrease and level off with the latter at about 30 years. This crossing point of the S-cone curve in [15] is well in accord with the age minimum of Tritan function found in the present study.

Beyond the threshold minima, the peak of chromatic sensitivity around 27–30 years, the present CCT measures reveal the onset of subtle deterioration of discrimination after age 40, as was found in our previous study [29]. This slow process, in statistical terms, is indicated by significant increases that are revealed when age cohort comparisons span three, not two life decades. Noteworthy, the slow-pace threshold increase affects initially the Tritan

system (cf. 20–29 vs. 40–49; Fig. 4c), to be followed by a similar process in the Protan and Deutan systems a decade later (cf. 30–39 vs. 50–59; Fig. 4a,b). Individual variability also noticeably increases starting from these life decades [cf. 9,10,49].

From 60 years onwards, a steeper threshold increase in all three chromatic systems is observed, coined the lifespan ‘knee’ by Haegerstrom-Portnoy et al. [9]. Our outcomes indicate though that the Protan system is least affected among the three systems, in accord with our previous findings that Protan discrimination losses are not serious earlier than in the 50–59 decade [29]. In comparison, the Deutan system appears to be more vulnerable at the upper extreme of the lifespan. Finally, the Tritan system undergoes fast-paced deterioration, with a noticeable ‘surge’ of senescence with each late life decade (Fig. 4c).

These findings are well in agreement with the Pokorny et al. [11] lens model, where a first slow phase of increase of lens density for the age under 60 years is followed by a faster second phase for ages older than 60. This is also apparent in the behavior of cone absorption functions, derived from the lens model, around the 60-year mark (Fig. 2; [15]); the ‘bend’ downwards is, however, significantly more prominent for S-cone absorption than for L- or M-cone absorption.

Age-related changes in the chromatic systems, in addition to the decline caused by ocular media, apparently reflect numerous neuronal changes [10]. This implies that considerable increase of the discrimination thresholds reflects deterioration processes of different etiology – senescence of the crystalline lens and losses in the neural pathways, in particular in the S-cone pathway that undergoes a greater decline of post-receptoral activity [19,22-24].

Acknowledgments

The study was supported by grants RES01400 and REF1011/20 from Liverpool Hope University. We thank John Mollon for the advice and Robert Hewertson for technical assistance. Indispensable help from Kenneth Knoblauch in estimating the fitting parameters of data distribution and support from David Bimler are gratefully appreciated. Contribution of Psychology students Simona Šiaulytė, Thomas Speight, Chandni Shyamdasani, Krishni Kunasingham, Ondrej Obediar, and Katie Robinson to data collection is gratefully acknowledged. The authors thank all participants for their time, understanding, and collaborative spirit. They are grateful to two anonymous reviewers for their constructive criticism that, in particular, ensured the accuracy of the power function parameters.

References

1. G. Verriest, J. Van Laethem, and A. Uvijls, "A new assessment of the normal ranges of the Farnsworth-Munsell 100-hue test scores," *Am. J. Ophthalmol.* **93**, 635–642 (1982).
2. G. Verriest, "Further studies on acquired deficiency of color discrimination," *J. Opt. Soc. Am.* **53**, 185–195 (1963).
3. K. J. Bowman, M. J. Collins, and C. J. Henry, "The effect of age on performance on the Panel D-15 and Desaturated D-15: A quantitative evaluation," *Colour Vision Deficiencies VII, Doc. Ophthalmol. Proc.* **39**, 227–231 (1984).
4. K. Knoblauch, F. Vital-Durand, and J. L. Barbur, "Variation of chromatic sensitivity across the life span," *Vision Res.* **41**, 23–36 (2001).
5. P. R. Kinnear, and A. Sahraie, "New Farnsworth-Munsell 100 hue test norms of normal observers for each year of age 5-22 and for age decades 30-70," *Brit. J. Ophthalmol.* **86**, 1408–1411 (2002).
6. D. F. Ventura, A. R. Rodrigues, A. A. Moura, A. C. Vargas, M. F. Costa, J. M. de Souza, and L. L. Silveira, "Color discrimination measured by the Cambridge Colour Vision Test (CCVT) in children and adults," *Invest. Ophthalmol. Vis. Sci.* **43**, E-Abstract 3796 (2002).
7. P. R. K. Goulart, M. L. Bandeira, D. Tsubota, N. N. Oiwa, M. F. Costa, and D. F. Ventura, "A computer-controlled color vision test for children based on the Cambridge Colour Test," *Vis. Neurosci.* **25**, 1–6 (2008).
8. J. S. Werner, D. H. Peterzell, and A. J. Scheetz, "Light, vision, and aging," *Optom. Vis. Sci.* **67**, 214–229 (1990).
9. G. Hagerstrom-Portnoy, M. E. Schneck, and J. A. Brabyn, "Seeing into old age: Vision function beyond acuity," *Optom. Vis. Sci.* **76**, 141–158 (1999).
10. J. S. Werner, "Visual problems of the retina during ageing: Compensation mechanisms and colour constancy across the life span," *Prog. Retin. Eye Res.* **15**, 621–645 (1996).

11. J. Pokorny, V. C. Smith, and M. Lutze, "Aging of the human lens," *Appl. Opt.* **26**, 1437–1440 (1987).
12. R. A. Weale, "Age and the transmittance of the human crystalline lens." *J. Physiol.* **395**, 577–587 (1988).
13. K. Okajima, and M. Takase, "Computerized simulation and chromatic adaptation experiments on a model of aged human lens." *Opt. Rev.* **8**, 64–70 (2001).
14. D. Nguyen-Tri, O. Overbury, and J. Faubert, "The role of lenticular senescence in age-related color vision changes," *Invest. Ophthalmol. Vis. Sci.* **44**, 3698–3704 (2003).
15. S. Wuerger, "Colour constancy across the life span: Evidence for compensatory mechanisms," *PLoS ONE* **8**(5): e63921 (2013). doi:10.1371/journal.pone.0063921
16. J. S. Werner, and V. G. Steele, "Sensitivity of human foveal color mechanisms throughout the life span," *J. Opt. Soc. Am. A* **5**, 2122–2129 (1988).
17. S. Wuerger, K. Xiao, C. Fu, and D. Karataz, "Colour-opponent mechanisms are not affected by age-related chromatic sensitivity changes," *Ophthal. Physiol. Opt.* **30**, 653–659 (2010).
18. C. Mateus, R. Lemos, M. F. Silva, A. Reis, P. Fonseca, B. Oliveiros, and M. Castelo-Branco, "Aging of low and high level vision: From chromatic and achromatic contrast sensitivity to local and 3D object motion perception." *PLoS ONE* **8**(1): e55348 (2013). doi:10.1371/journal.pone.0055348
19. C. A. Johnson, A. J. Adams, J. D. Twelker, and J. M. Quigg, "Age-related changes in the central visual field for short-wavelength-sensitive pathways," *J. Opt. Soc. Am. A* **5**, 2131–2139 (1988).
20. J. M. Kraft, and J. S. Werner, "Spectral efficiency across the life span: Flicker photometry and brightness matching," *J. Opt. Soc. Am. A* **11**, 1213–1221 (1994).

21. J. S. Werner, M. L. Bieber, and B. E. Schefrin, "Senescence of foveal and parafoveal cone sensitivities and their relations to macular pigment density," *J. Opt. Soc. Am. A* **17**, 1918–1932 (2000).
22. K. Shinomori, B. E. Schefrin, and J. S. Werner "Age-related changes in wavelength discrimination," *J. Opt. Soc. Am. A* **18**, 310–318 (2001).
23. M. B. Zlatkova, E. Coulter, and R. S. Anderson, "Short-wavelength acuity: blue–yellow and achromatic resolution loss with age," *Vision Res.* **43**, 109–115 (2003).
24. A. Werner, A. Bayer, G. Schwarz, E. Zrenner, and W. Paulus, "Effects of ageing on postreceptoral short-wavelength gain control: Transient tritanopia increases with age," *Vision Res.* **50**, 1641–1648 (2010).
25. J. D. Mollon, and B. C. Regan, *Cambridge Colour Test. Handbook* (Cambridge Research Systems Ltd., 2000). <http://visl.technion.ac.il/projects/2002w/theory.pdf>
26. B. C. Regan, J. P. Reffin, and J. D. Mollon, "Luminance noise and the rapid determination of discrimination ellipses in colour deficiency. *Vision Res.* **34**, 1279–1299 (1994).
27. D. L. MacAdam, "Visual sensitivities to color differences in daylight", *J. Opt. Soc. Am.* **32**, 247–274 (1942).
28. D. F. Ventura, L. C. L. Silveira, A. R. Rodrigues, J. M. De Souza, M. Gualtieri, D. Bonci, and M. F. Costa, "Preliminary norms for the Cambridge Colour Test", in *Normal & Defective Colour Vision*, J. D. Mollon, J. Pokorny, and K. Knoblauch, eds. (Oxford University Press, 2003), pp. 331–339.
29. G. V. Paramei, "Color discrimination across four life decades assessed by the Cambridge Colour Test," *J. Opt. Soc. Am. A* **29**, A290–A297 (2012).
30. B. C. Regan, N. Freudenthaler, R. Kollé, J. D. Mollon, and W. Paulus, "Colour discrimination thresholds in Parkinson's disease: Results obtained with a rapid computer-controlled colour vision test," *Vision Res.* **38**, 3427–3431 (1998).

31. M. P. Simunovic, M. Votruba, B. C. Regan, and J. D. Mollon, "Colour discrimination ellipses in patients with dominant optic atrophy," *Vision Res.* **38**, 3413–3419 (1998).
32. M. Castelo-Branco, P. Faria, V. Forjaz, L. R. Kozak, and H. Azevedo, "Simultaneous comparison of relative damage to chromatic pathways in ocular hypertension and glaucoma: Correlation with clinical measures," *Invest. Ophthalmol. Vis. Sci.* **45**, 499–505 (2004).
33. M. F. Silva, P. Faria, F. S. Regateiro, V. Forjaz, C. Januário, A. Freire, and M. Castelo-Branco, "Independent patterns of damage within magno-, parvo- and koniocellular pathways in Parkinson's disease," *Brain* **128**, 2260–2271 (2005).
34. D. F. Ventura, M. Gualtieri, M. F. Costa, P. Quiros, F. Sadun, A. M. de Negri, S. R. Salomão, A. Berezovsky, J. Sherman, A. A. Sadun, and V. Carelli, "Male prevalence of acquired color vision defects in asymptomatic carriers of Leber's hereditary optic neuropathy," *Invest. Ophthalmol. Vis. Sci.* **48**, 2362–2370 (2007).
35. C. Feitosa-Santana, M. T. S. Barboni, N. N. Oiwa, G. V. Paramei, A. L. Simões, M. F. Costa, L. C. L. Silveira, and D. F. Ventura, "Irreversible color vision losses in patients with chronic mercury vapor intoxication," *Vis. Neurosci.* **25**, 487–491 (2008).
36. A. L. D. A. Moura, R. A. A. Teixeira, N. N. Oiwa, M. F. Costa, C. Feitosa-Santana, D. Callegaro, R. D. Hamer, and D. F. Ventura, "Chromatic discrimination losses in multiple sclerosis patients with and without optic neuritis using the Cambridge Colour Test," *Vis. Neurosci.* **25**, 463–468 (2008).
37. C. Feitosa-Santana, G. V. Paramei, M. Nishi, M. Gualtieri, M. F. Costa, and D. F. Ventura, "Color vision impairment in type 2 diabetes assessed by the D-15d test and the Cambridge Colour Test," *Ophthalm. Physiol. Opt.* **30**, 717–723 (2010).
38. A. Reis, C. Mateus, M. C. Macário, J. R. F. de Abreu, and M. Castelo-Branco, "Independent patterns of damage to retinocortical pathways in multiple sclerosis without a previous episode of optic neuritis," *J. Neurol.* **258**, 1695–1704 (2011).

39. S. Ishihara, *Test for Colour-Blindness*, 24 Plates Edition (Kanehra Shupan Co., Ltd., 1973).
40. D. Farnsworth, “Farnsworth-Munsell 100-Hue and Dichotomous test for color vision,” *J. Opt. Soc. Am.* **33**, 568–578 (1943).
41. P. Lanthony, “The Desaturated Panel D-15,” *Doc. Ophthalmol.* **46**, 185–189 (1978).
42. D. de Fez, J. Luque, and V. Viqueira, “Enhancement of contrast sensitivity and losses of chromatic discrimination with tinted lenses,” *Optom. Vis. Sci.* **79**, 590–597 (2002).
43. Cambridge Research Systems Ltd., <http://www.crsLtd.com/tools-for-vision-science/measuring-visual-functions/cambridge-colour-test/>
44. K. Knoblauch, and L. T. Maloney, *Modeling Psychophysical Data in R* (Springer, 2012), Ch. 2, pp. 45–56.
45. K. Krishnamoorthy, *Handbook of Statistical Distributions with Applications* (Chapman and Hall/CRC, 2006), pp. 323–324.
46. STATGRAPHICS Centurion: <http://www.statgraphics.com>
47. M. F. Costa, D. F. Ventura, F. Perazzolo, M. Murakoshi, and L. C. L. Silveira, “Absence of binocular summation, eye dominance, and learning effects in color discrimination,” *Vis. Neurosci.* **23**, 461–469 (2006).
48. J. K. Hovis, “Comparison of three computer based color vision tests,” *Aviation Space Environ. Med.* **82**, 243 (2011).
49. A. Panorgias, Department of Ophthalmology & Vision Science, University of California Davis, 4860 Y street, Sacramento, CA, 95816, USA, K. Shinomori, J. M. Kelly, and J. S. Werner are preparing a manuscript to be called “Changes in chromatic discrimination thresholds over seven decades of life.”

Appendix

Tables A1, A2 here

Table 1. Participant number of both genders (F=females, M=males) and age details (y.o.) for each age band

Statistics	10+	20+	30+	40+	50+	60+	70+	80+
Gender split	20F, 20M	20F, 20M	20F, 20M	20F, 20M	20F, 20M	20F, 20M	18F, 17M	12F, 4M
Mean (SD)	14.8 (2.9)	22.6 (2.8)	33.3 (2.8)	43.3 (2.7)	54.0 (2.8)	64.2 (3.0)	74.4 (2.8)	82.3 (2.4)

Table 2. Trivector ($10^{-4} u'v'$ units): Median, Half-Interquartile Range (IQR/2) and Tolerance Limits for eight life decades

<i>Protan vector</i>								
Statistics	10+	20+	30+	40+	50+	60+	70+	80+
Median (IQR/2)	51.0 (12)	40.0 (6.5)	40.5 (7.0)	41.5 (10.0)	46.0 (7.5)	53.5 (13.5)	56.0 (14.0)	63.0 (24.5)
Upper limit	92	64	64	77	82	116	98*	171**
Lower limit	26	23	23	26	26	29	35*	33**
<i>Deutan vector</i>								
Statistics	10+	20+	30+	40+	50+	60+	70+	80+
Median (IQR/2)	48.5 (11.5)	40.5 (10.0)	38.5 (7.5)	46.0 (10.5)	46.0 (11.0)	54.0 (12.0)	62.0 (13.5)	75.0 (23.0)
Upper limit	101	69	65	80	127	109	150*	116**
Lower limit	26	26	23	26	26	29	26*	38**
<i>Tritan vector</i>								
Statistics	10+	20+	30+	40+	50+	60+	70+	80+
Median (IQR/2)	57.0 (13.5)	53.0 (8.0)	58.0 (9.0)	64.0 (14.5)	65.0 (14.5)	82.0 (25)	119.0 (35)	188.0 (62)
Upper limit	119	95	169	130	159	139	333*	428**
Lower limit	29	26	23	27	33	45	40*	59**

* Range valid for 90% of the population, estimated probability 88%; ** Range valid for 80% of the population, estimated probability 86%.

Table 3. Summary of parameter fits to Eq. (1)

Vector	<i>a</i>	α	<i>b</i>	β	A_{\min} (years)	R^2
Protan	24.25 (9.59)	-0.59 (0.30)	16.94 (9.84)	1.50 (0.60)	30	.23
Deutan	23.19 (9.98)	-0.62 (0.30)	18.08 (9.37)	1.52 (0.55)	29	.23
Tritan	54.74 (2.88)	-0.027 (0.076)	2.16 (1.40)	5.44 (0.91)	27	.45

Table 4. Ellipses test, Length of the Major Axis ($10^{-5} u'v'$ units): Median, Half-Interquartile Range (IQR/2) and Tolerance Limits for eight life decades

<i>Ellipse 1</i>								
Statistics	10+	20+	30+	40+	50+	60+	70+	80+
Median (IQR/2)	137.0 (23.5)	106.5 (15.5)	112.5 (15.0)	116.5 (19.5)	124.5 (30.0)	154.0 (35.5)	247.0 (71.0)	387.0 (251.0)
Upper limit	195	221	192	241	287	631	797*	958**
Lower limit	76	77	80	69	84	96	117*	161**
<i>Ellipse 2</i>								
Statistics	10+	20+	30+	40+	50+	60+	70+	80+
Median (IQR/2)	154.5 (32.0)	118.5 (20.5)	130.5 (20.0)	144.5 (28.0)	154.0 (34.5)	215.5 (71.0)	380.0 (93.5)	416.0 (182.5)
Upper limit	306	203	242	295	363	541	1252*	936**
Lower limit	102	75	76	86	102	115	107*	229**
<i>Ellipse 3</i>								
Statistics	10+	20+	30+	40+	50+	60+	70+	80+
Median (IQR/2)	199.8 (32.5)	157.5 (35.5)	150.0 (29.0)	179.0 (49.5)	192.5 (59.5)	215.5 (85.5)	284.0 (128.0)	413.0 (182.0)
Upper limit	559	286	439	387	421	468	751*	1639**
Lower limit	113	97	101	99	106	109	122*	210**

* Range valid for 90% of the population, estimated probability 88%; ** Range valid for 80% of the population, estimated probability 86%.

Table 5. Ellipses test, Major-to-Minor Axis Ratio: Median, Half-Interquartile Range (IQR/2) and Tolerance Limits for eight life decades

<i>Ellipse 1</i>								
Statistics	10+	20+	30+	40+	50+	60+	70+	80+
Median (IQR/2)	1.39 (.15)	1.29 (.17)	1.31 (.20)	1.37 (.19)	1.43 (.31)	1.46 (.29)	2.05 (.67)	2.84 (.78)
Upper limit	2.26	2.66	2.43	3.47	2.86	5.89	6.25*	10.77**
Lower limit	1.02	1.07	1.03	1.03	1.11	1.10	1.30*	1.65**
<i>Ellipse 2</i>								
Statistics	10+	20+	30+	40+	50+	60+	70+	80+
Median (IQR/2)	1.47 (.22)	1.34 (.15)	1.33 (.23)	1.42 (.22)	1.42 (.19)	1.69 (.36)	2.69 (.63)	2.70 (.69)
Upper limit	2.44	2.22	2.46	2.53	3.68	3.66	8.87*	5.60**
Lower limit	1.10	1.04	1.08	1.03	1.06	1.20	1.10*	1.60**
<i>Ellipse 3</i>								
Statistics	10+	20+	30+	40+	50+	60+	70+	80+
Median (IQR/2)	1.87 (.25)	2.09 (.36)	1.86 (.36)	2.08 (.50)	2.04 (.46)	2.27 (.72)	2.51 (.80)	2.65 (1.61)
Upper limit	4.59	3.10	4.25	4.90	5.32	3.77	7.72*	12.26**
Lower limit	1.13	1.13	1.04	1.26	1.33	1.12	1.46*	1.18**

* Range valid for 90% of the population, estimated probability 88%; ** Range valid for 80% of the population, estimated probability 86%.

Table 6. Ellipses test, Angle of the Major Axis (deg): Median, Half-Interquartile Range (IQR/2) and Tolerance Limits for eight life decades

<i>Ellipse 1</i>								
Statistics	10+	20+	30+	40+	50+	60+	70+	80+
Median (IQR/2)	72.7 (26.3)	66.7 (15.5)	79.7 (19.8)	81.6 (19.7)	76.2 (19.0)	77.1 (12.6)	86.1 (8.8)	84.7 (4.4)
Upper limit	178	158	174	172	168	137	119*	104**
Lower limit	0	6	11	3	20	12	21*	60**
<i>Ellipse 2</i>								
Statistics	10+	20+	30+	40+	50+	60+	70+	80+
Median (IQR/2)	83.9 (40.0)	87.4 (23.5)	83.5 (38.9)	90.2 (28.0)	81.4 (17.8)	84.5 (17.6)	90.2 (9.1)	89.4 (5.0)
Upper limit	168	179	178	179	175	166	154*	107**
Lower limit	0	0	8	0	30	8	11*	75**
<i>Ellipse 3</i>								
Statistics	10+	20+	30+	40+	50+	60+	70+	80+
Median (IQR/2)	98.9 (9.6)	95.5 (8.3)	97.9 (8.4)	96.0 (8.8)	96.1 (9.4)	96.5 (5.4)	89.5 (7.5)	90.2 (8.3)
Upper limit	173	161	130	129	109	152	120*	139**
Lower limit	30	52	69	58	69	59	78*	79**

* Range valid for 90% of the population, estimated probability 88%; ** Range valid for 80% of the population, estimated probability 86%.

Appendix

**Table A1. Ellipses test, Length of the Major Axis: Mann-Whitney U for first significant difference between life decades.
In each cell, for Ellipse 1: top row; Ellipse 2: middle row; Ellipse 3: bottom row**

Decade	10+	20+	30+	40+	50+	60+	70+
20+		396.5, $p<.001$					
		339.5, $p<.001$					
		(628.5, $p=.099$)					
40+		428.0, $p<.001$					
		(607.5, $p=.064$)					
50+			567.0, $p=.025$				
60+					519.5, $p=.007$		
					418.5, $p<.001$		
				548.0, $p=.015$			
70+						310.5, $p<.001$	
						265.5, $p<.001$	
						486.5, $p=.023$	
80+							134.0, $p=.003$
						92.5, $p<.001$	
							169.5, $p=.025$

**Table A2. Ellipses test, Major-to-minor axis ratio: Mann-Whitney U for first significant difference between life decades.
In each cell, for Ellipse 1: top row; Ellipse 2: middle row; Ellipse 3: bottom row**

Decade	10+	20+	30+	40+	50+	60+	70+
50+	588.0, $p=.041$						
	582.0, $p=.036$						
60+	448.0, $p=.001$						
70+						350.0, $p<.001$	
						280.0, $p<.001$	
						508.0, $p=.041$	
80+						76.0, $p<.001$	169.0, $p=.024$
						97.0, $p<.001$	
						198.0, $p=.018$	

Figure legends

Fig. 1. An illustration of the chromatic targets, Landolt 'C', embedded in the luminance noise background. [Source: J. D. Mollon and B. C. Regan, *Cambridge Colour Test. Handbook* (Cambridge Research Systems Ltd., 2000), p. 4].

Fig. 2. (a) Protan (P), Deutan (D) and Tritan (T) vectors (in CIE 1976 $u'v'$ color space) along which the chromaticity is varied in the CCT Trivector test. The origin of the vectors indicates chromaticity coordinates of the neutral background ($u' = 0.1977$, $v' = 0.4689$). The monitor gamut is represented by the white triangle. [Source: M. F. Silva et al., "Independent patterns of damage within magno-, parvo- and koniocellular pathways in Parkinson's disease," *Brain* **128** (2005), p. 2265.] (b) Examples of chromatic discrimination ellipses for young adult normal trichromats: Ellipse 1 (middle), Ellipse 2 (top), Ellipse 3 (bottom); crosses indicate raw discrimination vectors, fitted ellipses are shown by solid lines. [Source: J. D. Mollon and B. C. Regan, *Cambridge Colour Test. Handbook* (Cambridge Research Systems Ltd., 2000), Graph 1].

Fig. 3. Trivector test: Ln of chromatic discrimination thresholds ($10^{-4} u'v'$ units) along the Protan (left), Deutan (middle) and Tritan (right) axes as a function of age. The solid curve is the best fit of Eq. (1) to the data. The values of R^2 indicate variance accounted for by the fitted curves.

Fig. 4. Trivector test: Ln of chromatic discrimination thresholds ($10^{-4} u'v'$ units) along the (a) Protan, (b) Deutan, and (c) Tritan axes for the eight life decades. Significant differences between the age bands are indicated by horizontal lines accompanied by corresponding p -values.

Fig. 5. Ellipses test, Ellipse 1: Ln of the (a) Length of the major axis ($10^{-5} u'v'$ units) and (b) Major-to-minor axis ratio for the eight life decades.

Figure 1

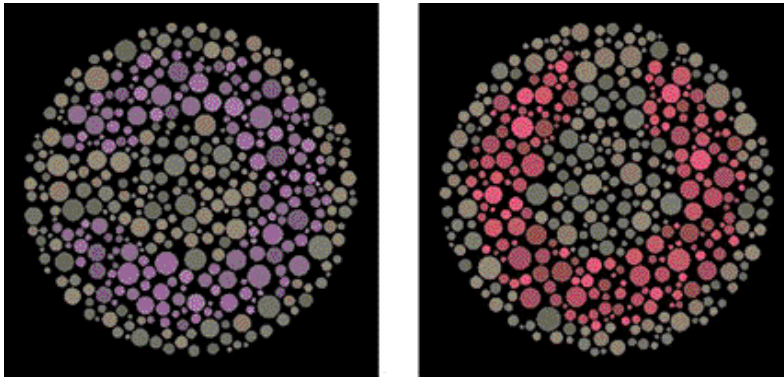


Figure 2

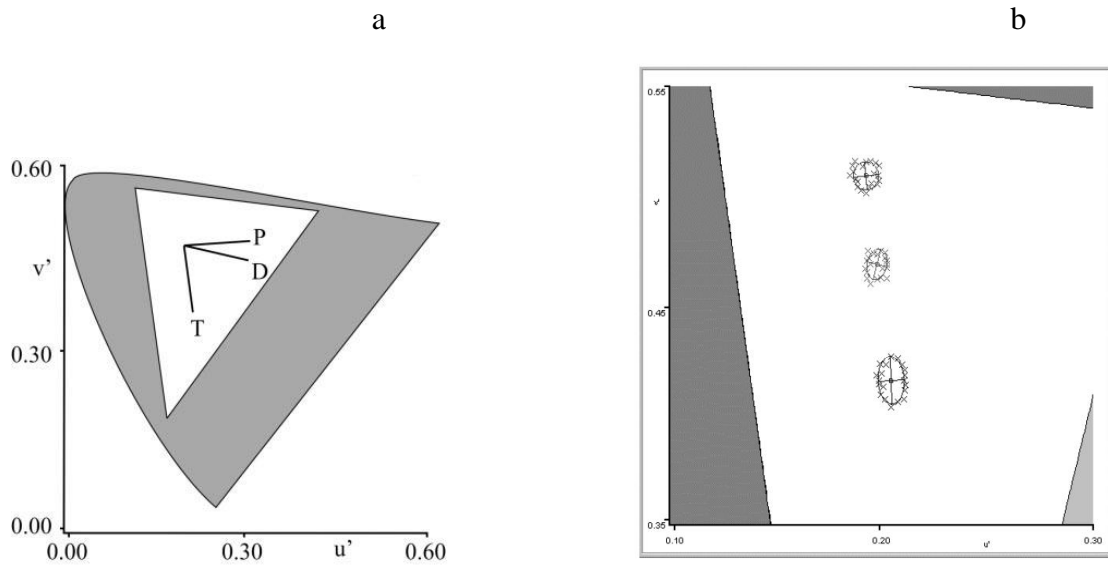


Figure 3

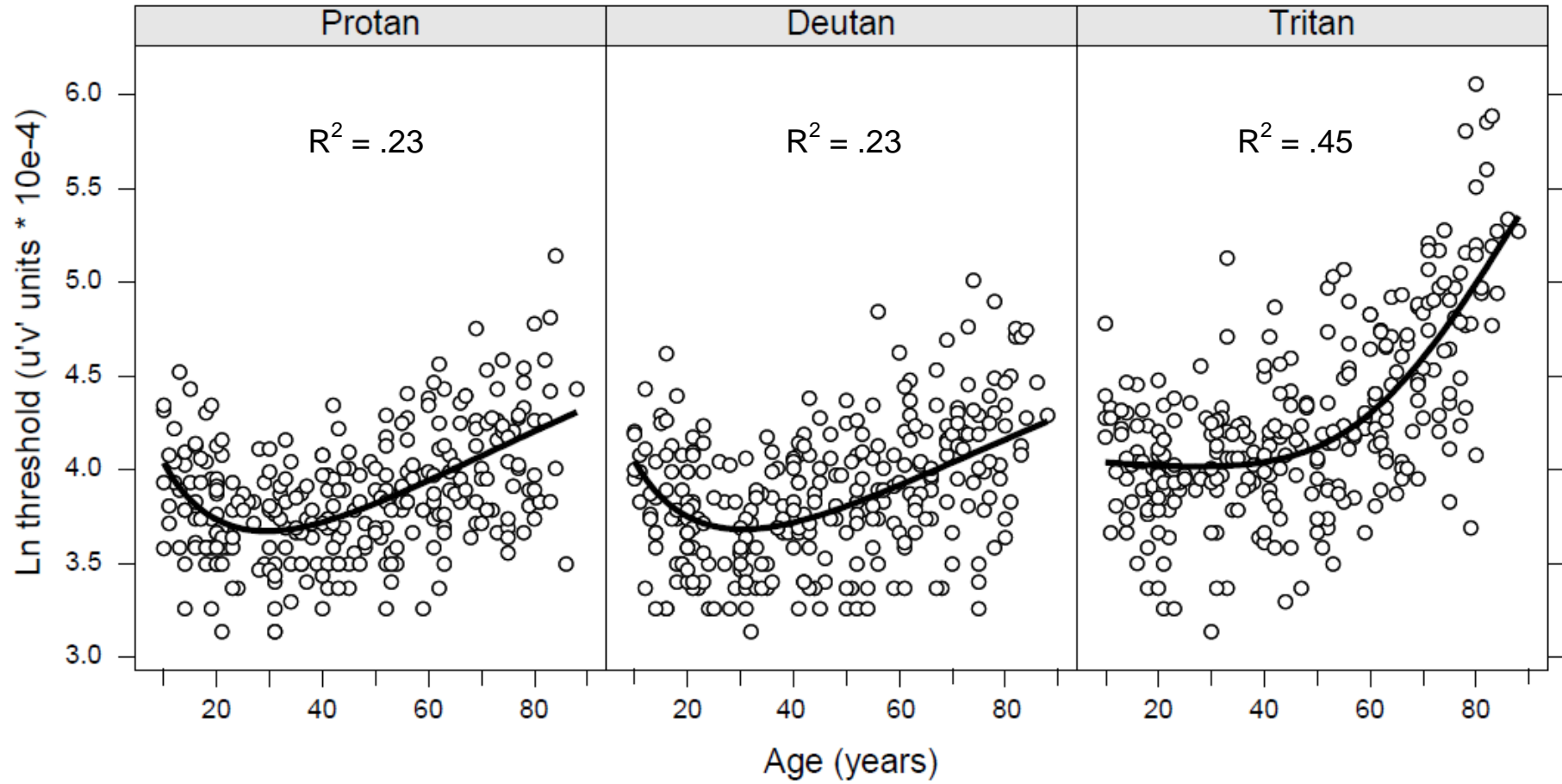


Figure 4a

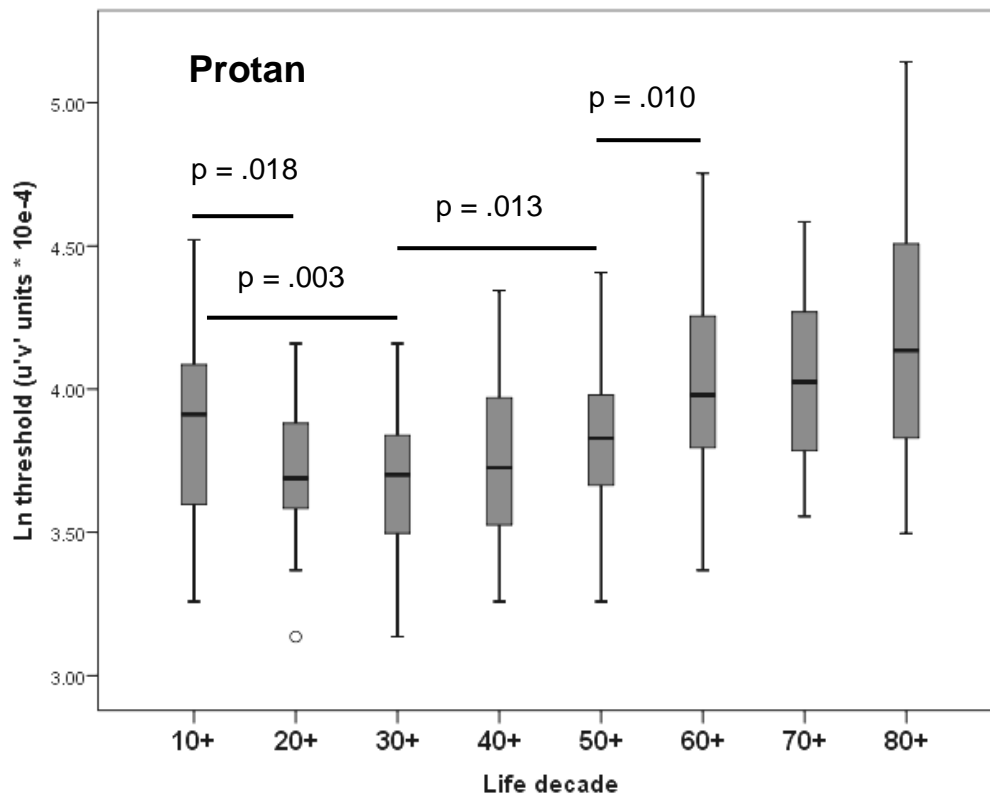


Figure 4b

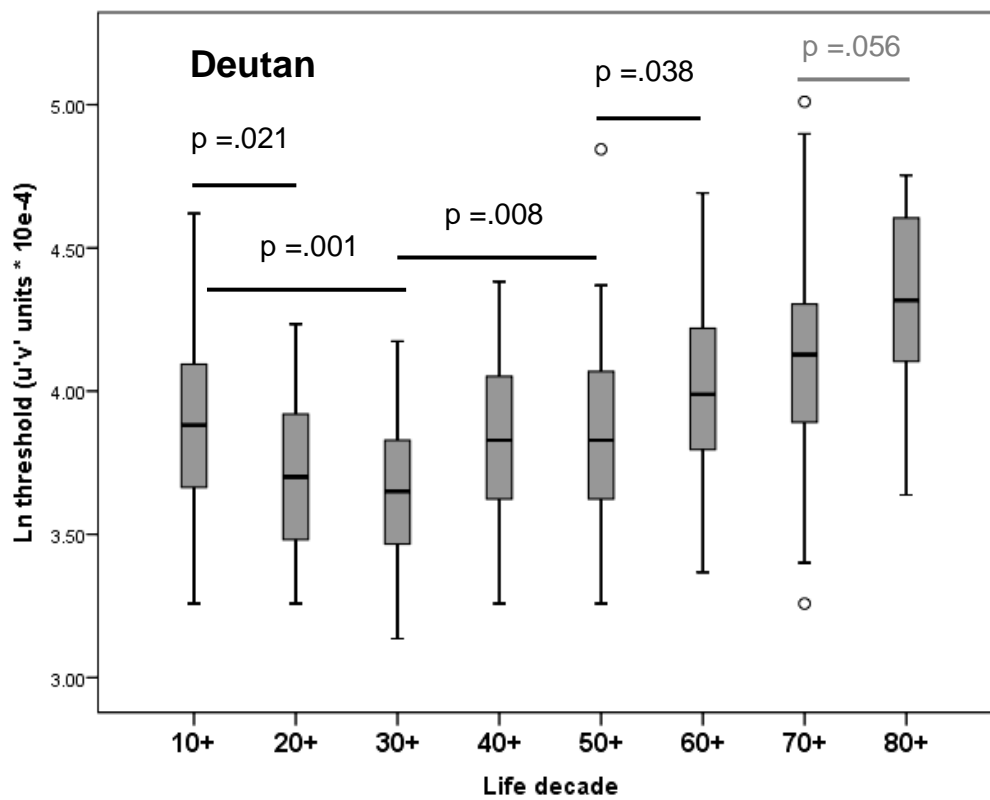


Figure 4c

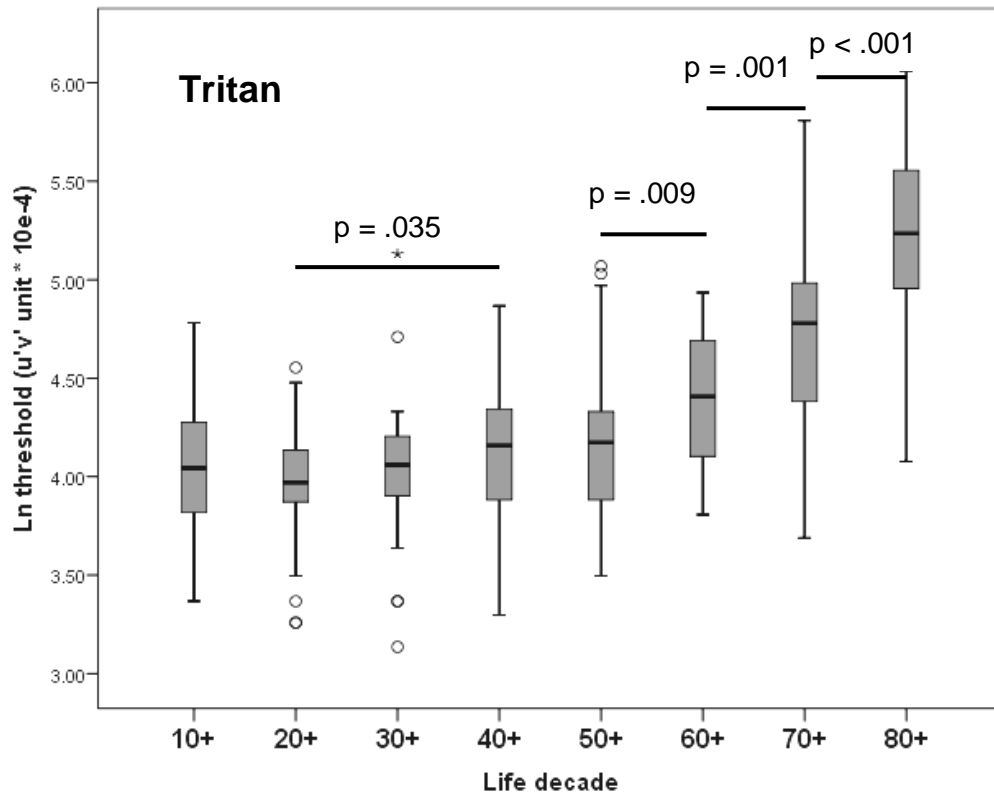


Figure 5a

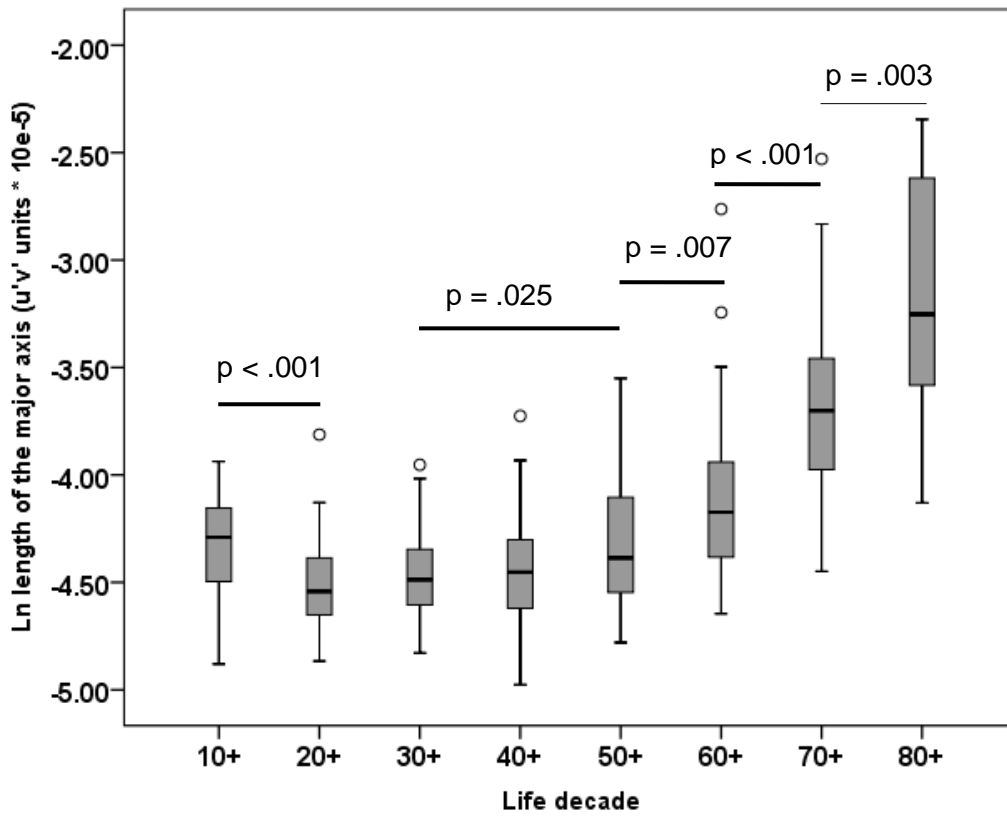


Figure 5b

